JGR Oceans

RESEARCH ARTICLE
10.1029/2021JC018275

Local and Remote Forcing of Interannual Sea-Level Variability at Nantucket Island

Ou Wang[1], Tong Lee[1], Christopher G. Piecuch[2], Ichiro Fukumori[1], Ian Fenty[1], Thomas Frederikse[1,3], Dimitris Menemenlis[1], Rui M. Ponte[4], and Hong Zhang[1]

[1]Jet Propulsion Laboratory, California Institute of Technology, Pasadena, CA, USA, [2]Physical Oceanography Department, Woods Hole Oceanographic Institution, Woods Hole, MA, USA, [3]Joint Institute for Regional Earth System Science and Engineering, University of California, Los Angeles, CA, USA, [4]Atmospheric and Environmental Research, Inc., Lexington, MA, USA

Key Points:

- We establish causality of Nantucket interannual sea-level variations with local and remote atmospheric forcings using a rigorous approach
- Local wind forcing has larger contribution than remote winds, while remote buoyancy forcing is more important than local buoyancy forcing
- Subpolar buoyancy forcing can significantly influence Nantucket sea level a few years later, affecting Nantucket sea-level predictability

Supporting Information:

Supporting Information may be found in the online version of this article.

Correspondence to:

T. Lee,
tlee@jpl.nasa.gov

Citation:

Wang, O., Lee, T., Piecuch, C. G., Fukumori, I., Fenty, I., Frederikse, T., et al. (2022). Local and remote forcing of interannual sea-level variability at Nantucket Island. *Journal of Geophysical Research: Oceans*, *127*, e2021JC018275. https://doi.org/10.1029/2021JC018275

Received 24 NOV 2021
Accepted 2 JUN 2022

Author Contributions:

Conceptualization: Ou Wang, Tong Lee, Ichiro Fukumori
Data curation: Ou Wang
Formal analysis: Ou Wang, Tong Lee, Christopher G. Piecuch
Funding acquisition: Tong Lee
Investigation: Ou Wang, Tong Lee, Christopher G. Piecuch, Ichiro Fukumori, Ian Fenty, Thomas Frederikse, Dimitris Menemenlis, Rui M. Ponte, Hong Zhang
Methodology: Ou Wang, Tong Lee, Christopher G. Piecuch, Ichiro Fukumori

Abstract The relative contributions of local and remote wind stress and air-sea buoyancy forcing to sea-level variations along the East Coast of the United States are not well quantified, hindering the understanding of sea-level predictability there. Here, we use an adjoint sensitivity analysis together with an Estimating the Circulation and Climate of the Ocean (ECCO) ocean state estimate to establish the causality of interannual variations in Nantucket dynamic sea level. Wind forcing explains 67% of the Nantucket interannual sea-level variance, while wind and buoyancy forcing together explain 97% of the variance. Wind stress contribution is near-local, primarily from the New England shelf northeast of Nantucket. We disprove a previous hypothesis about Labrador Sea wind stress being an important driver of Nantucket sea-level variations. Buoyancy forcing, as important as wind stress in some years, includes local contributions as well as remote contributions from the subpolar North Atlantic that influence Nantucket sea level a few years later. Our rigorous adjoint-based analysis corroborates previous correlation-based studies indicating that sea-level variations in the subpolar gyre and along the United States northeast coast can both be influenced by subpolar buoyancy forcing. Forward perturbation experiments further indicate remote buoyancy forcing affects Nantucket sea level mostly through slow advective processes, although coastally trapped waves can cause rapid Nantucket sea level response within a few weeks.

Plain Language Summary The change in the rate of sea-level rise (SLR) in the northeast coast of the United States in the past few decades was 3–4 times higher than that of the global-mean SLR. The magnitude of interannual sea-level variation in this region is even larger than the long-term change over the last few decades. The causes of interannual sea-level variation there are not well understood, limiting the knowledge of sea-level predictability. This study identifies the causality of interannual variations of sea level near Nantucket Island with wind and buoyancy forcing. The latter is the combination of air-sea heat and freshwater fluxes. These forcings together affect sea level. We employ a method to separate the contributions of wind and buoyancy forcings, both near and away from Nantucket, on Nantucket sea level. Wind contribution is primarily near-local, from regions northeast of Nantucket along the New England shelf. Local and remote buoyancy forcing contributions are overall smaller than wind contributions, but can be comparable to wind contributions in some years. In particular, buoyancy forcing from the subpolar North Atlantic can affect Nantucket sea level a few years later, providing a source of predictability for Nantucket sea level.

1. Introduction

The northeast coast of the United States (US) is a densely-populated region with enhanced sea level rise (SLR) relative to the global mean (Sallenger et al., 2012). Many processes contribute to sea-level change in this region (Little et al., 2019; Woodworth et al., 2019 and references therein). Quantifying the relative contributions of these different processes to past sea-level change can improve the reliability of future SLR predictions.

The magnitude of interannual sea-level variations in the northeast US is large compared to the long-term secular trend over the last few decades (Andres et al., 2013). For example, Goddard et al. (2015) reported an extreme seal-level variation during 2009–2010 that was equivalent to approximately 30 years of global-mean SLR. In addition to having large magnitudes, interannual sea-level variations in the region are also coherent from Cape

Project Administration: Tong Lee
Resources: Tong Lee
Software: Ou Wang
Supervision: Tong Lee
Validation: Ou Wang
Visualization: Ou Wang
Writing – original draft: Ou Wang, Tong Lee, Christopher G. Piecuch
Writing – review & editing: Ou Wang, Tong Lee, Christopher G. Piecuch, Ichiro Fukumori, Ian Fenty, Thomas Frederikse, Dimitris Menemenlis, Rui M. Ponte, Hong Zhang

Hatteras to Nova Scotia (Figure S1; Andres et al., 2013; Thompson, 1986; McCarthy et al., 2015; Thompson & Mitchum, 2014; Woodworth et al., 2014; Piecuch et al., 2016; Little et al., 2021).

Many past studies have argued that local wind forcing is the dominant driver of interannual sea-level variations in the northeast US coast (Andres et al., 2013; Piecuch et al., 2016, 2019; Woodworth et al., 2014, 2017). However, Chen et al. (2020) stated that local along-shore wind stress only explains 5% of the variance of the interannual sea-level variations in the Mid-Atlantic Bight and about 30% of the variance along the Nova Scotia Coast. Remote forcing has also been hypothesized to be an important contributor. For instance, Frederikse et al. (2017) found a strong correlation between steric height in the subpolar gyre and the sea level along the US northeast coast on decadal timescales, implicating a common forcing for both.

These previous studies were either based on correlation analysis (e.g., Andres et al., 2013) or highly simplified models (e.g., Piecuch et al., 2016). Correlation or regression analyses cannot establish causality. More advanced models can confirm or invalidate previous findings based on simplified models. In this study, we establish causality by employing a rigorous method based on the state estimation framework developed by the consortium for Estimating the Circulation and Climate of the Ocean (ECCO), in particular, sea-level sensitivities to forcings computed by the adjoint model derived from the ECCO forward model (hereafter ECCO adjoint model).

We aim to establish causality between interannual sea-level variations near Nantucket Island off the US northeast coast with local and remote wind stress and buoyancy forcings. Local forcings are defined as those over the Gulf of Maine (GoM; Figure S1). Remote forcings are defined as those in more distant regions including the subpolar North Atlantic. In particular, we analyze Nantucket sea-level sensitivities to forcings, which depict Nantucket sea-level response to unit perturbations of the forcings, and the convolution of the sensitivities with forcings. The analysis decomposes Nantucket sea-level variations into contributions from individual forcings from various regions and different lead times so as to quantify the relative importance of local and remote forcings. The causality analysis helps verify or nullify previous hypotheses that were based on correlation analyses or simple models of the roles of these forcings.

The paper is organized as follows. The model and methodology are described in Section 2. In Section 3, we present the adjoint-based reconstruction of Nantucket sea level. We investigate the local and remote forcing contributions to Nantucket sea level in Section 4. Two events of enhanced buoyancy forcing contributions are studied in detail in Section 5. Using perturbation experiments, we investigate how remote buoyancy forcing and wind stress in different regions affect Nantucket sea level in Section 6. Finally, we give concluding remarks in Section 7.

2. Model and Methodology

Because seasonal-to-decadal sea-level variations are coherent north of Cape Hatteras from Mid-Atlantic Bight to GoM (Figure S1 or see Andres et al., 2013), we choose to use sea level at Nantucket Island as a proxy for sea level along the entire US northeast coast. Nantucket is also the approximate geographic center of the US northeast coast region. The model grid cell that we define as "Nantucket" is at 41.4°N, 70.5°W, with 20-m model water depth.

We focus on interannual sea-level variations during 1992–2015 and use the global, data-constrained ECCO Version 4 Release 3 (hereafter ECCO V4r3) ocean and sea-ice estimate (Forget et al., 2015; Fukumori et al., 2017). As there is no surface atmospheric pressure loading in the ECCO V4r3 solution, sea level in this study refers to ocean dynamic sea level without the inverse barometer (IB) effect. The IB effect accounts for 25% of interannual variance of total sea level along the US northeast coast (Piecuch & Ponte, 2015).

The ECCO state estimates are obtained by fitting the Massachusetts Institute of Technology general circulation model (MITgcm) to satellite and in-situ ocean and sea-ice observations using an adjoint-based optimization method. The model's first-guess surface boundary conditions, initial conditions, and mixing parameters are iteratively adjusted to minimize the model-data differences in a least-squares sense. The time-trajectory of the optimized, free-running model can be entirely ascribed to first principles, namely, satisfying the physics described by the model equations. Covering the period 1992–2015, the ECCO V4r3 solution has a nominal 1° horizontal grid spacing and 50 vertical levels with thickness varying from 10 m near the surface to 456.5 m at a maximum depth of 6,134.5 m. The model uses a rescaled vertical coordinate z*, a non-linear free surface, and real freshwater flux boundary condition. They help the numerical model accurately account for the mass and

density contributions to sea level by material exchanges through the ocean surface (Campin et al., 2008; Forget et al., 2015). Numerous studies have used various ECCO products to investigate changes in sea level (e.g., Forget & Ponte, 2015; Schloesser et al., 2021), temperature and salinity (e.g., Liu et al., 2019; Ponte et al., 2021; Ponte & Piecuch, 2018), and other oceanic physical properties. A comprehensive list of ECCO-related publications can be found at https://ecco-group.org/publications.htm.

To quantify the relative contribution of different forcing from different locations to Nantucket sea-level variations, we employ the method of adjoint gradient decomposition (Fukumori et al., 2015) whereby a quantity of interest (objective function), Nantucket sea level in this case, is expanded linearly in terms of its causal elements using the ECCO adjoint model. While the original ECCO V4r3 solution uses time-evolving atmospheric state and bulk formulae to calculate the individual air-sea heat and freshwater flux terms (e.g., sensible and latent heat flux, evaporation), this study employs a "flux-forced" version of the ocean model forced with prescribed zonal and meridional wind stress (TAUU and TAUV), net heat flux (QNET), and net freshwater flux (EmPmR) of V4r3 that allows the influences of different forcing mechanisms to be more readily quantified (Fukumori et al., 2021).

We run the ECCO adjoint model backward in time to calculate the adjoint sensitivities of Nantucket sea level with respect to these four air-sea fluxes as a function of location and lead time. Specifically, sensitivities are calculated using monthly-mean Nantucket sea level in December 2015 as the objective function, thus allowing the computation of adjoint sensitivities to forcings with the longest possible lead time over the 1992–2015 ECCO V4r3 period. The resultant set of adjoint sensitivities quantifies the linear response of Nantucket sea level to unit positive perturbations in each forcing as a function of location and lead time. We make a reasonable approximation that the adjoint sensitivities are independent from ocean state and therefore stationary in time, following previous studies (e.g., Heimbach et al., 2011; Kostov et al., 2021; Pillar et al., 2016; Smith & Heimbach, 2019; Verdy et al., 2014).

Figure 1 shows adjoint sensitivities of Nantucket sea level to heat flux, freshwater flux, zonal and meridional wind stress at various forcing lead times. The values have been normalized by the maximum sensitivity value in the region (number specified on each panel) and are thus non-dimensional. The heat and freshwater flux sensitivities at 1-year lead time are mostly from the Scotian Shelf that is not very far from Nantucket Island. As the lead time increases, the largest sensitivities occur in regions farther away, for example, from the subpolar North Atlantic with forcing lead times of 2–3 years and south of Iceland at year 5. In contrast, the wind stress sensitivities are dominated by local features and even going back further in time, the largest sensitivities are still not very far from Nantucket Island.

To reconstruct Nantucket sea-level anomaly (SLA) at a target time, t, the adjoint sensitivities are convolved with the anomalies of each forcing with respect to its time mean. Mathematically, Nantucket SLA, J, is reconstructed by the following equation:

$$J(t) \approx \sum_i \sum_s \sum_{\Delta t} \frac{\partial J}{\partial F_i(s,\Delta t)} \delta F_i(s, t-\Delta t) \tag{1}$$

where $\frac{\partial J}{\partial F_i(s,\Delta t)}$ is the adjoint sensitivity of Nantucket SLA to forcing F_i at lead time Δt and location s; and $\delta F_i(s, t-\Delta t)$ is the anomaly of forcing F_i at some prior time $t-\Delta t$ (i.e., target time minus lead time).

Using Equation 1, one can reconstruct Nantucket SLA time series by aggregating the cumulative contributions of all forcings through all lead time and space. To gain insight into the contributions of particular forcings to the overall sea-level variation, we analyze the individual elements of Equation 1. In fact, this is the basis for us to decipher the relative contributions of different forcings as well as local versus remote forcings. See Fukumori et al. (2007, 2015, 2021) for details regarding the methodology of the decomposition and reconstruction to determine causal mechanisms.

Unless otherwise specified, the study is based on 13-month low-pass-filtered monthly sea-level time series, referenced to its global and 1992–2015 time means, with the seasonal cycle and a linear trend removed so as to focus on regional interannual variations. We show that the convolution-based sea-level reconstruction reproduces most of the interannual sea-level variance at Nantucket estimated by ECCO. We then decompose the reconstructed Nantucket sea-level variations into individual forcing contributions or regional contributions.

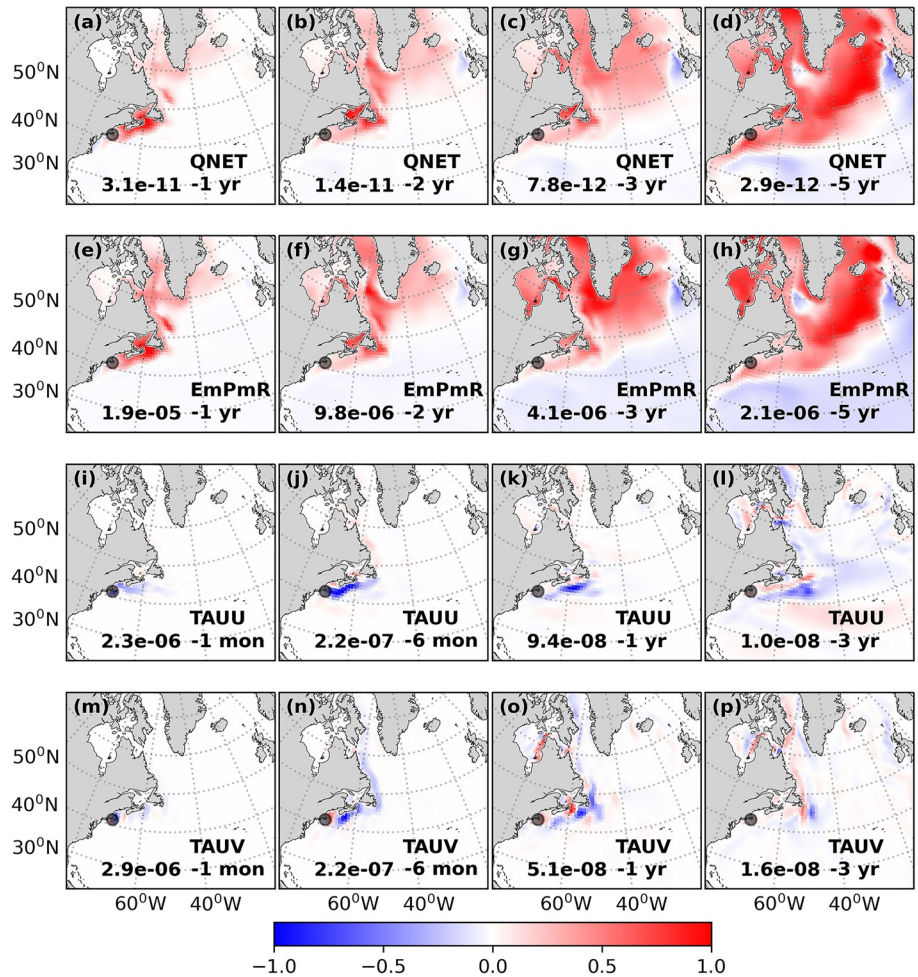

Figure 1. Nantucket sea-level sensitivity to heat flux (a)–(d), freshwater flux (e)–(h), zonal (i)–(l) and meridional wind stress (m)–(p) at various forcing lead times (indicated by legends) computed by integrating the ECCO adjoint model backward in time. The circle indicates the location near Nantucket Island where the objective function is defined. For each panel, the values of the sensitivities have been normalized by the maximum magnitude of sensitivities in the region (shown in legends) and are thus non-dimensional. Positive sensitivity value at a location means that a positive perturbation to the forcing at that location for the particular lead time will increase Nantucket sea level at the terminal time (time 0). The sign convention for the forcing itself is positive for downward heat flux (W m^{-2}) and freshwater flux (kg m^{-2} s^{-1}), eastward and northward wind stress (N m^{-2}). Longer lead times are shown for the sea-level sensitivities to heat and freshwater fluxes because of the longer time scales of their evolutions.

3. Adjoint-Based Reconstruction of Nantucket Sea Level

Figure 2a compares interannual variations of Nantucket sea level estimated by ECCO (blue) to tide-gauge data (gray) and the estimate from the Archiving, Validation and Interpretation of Satellite Oceanographic (AVISO) merged-altimetry gridded product (black). Both tide-gauge data and AVISO have been corrected for the IB effect and are referenced to global-mean sea level from AVISO. The tide-gauge SLA are very similar to the AVISO SLA even though the latter have been spatially averaged onto the ECCO grid closest to Nantucket. While ECCO estimate overall resembles these observations (correlation coefficient $r = 0.79$ and 0.80, respectively), there are some notable mismatches, for example, during 1997 and 2013. These mismatches are likely due to limitations in the ECCO V4r3 model (e.g., coarse grid resolution and representation of coastal processes), because the tide-gauge data is more similar to AVISO ($r = 0.93$) despite some notable difference between them. The reconstructed Nantucket sea level (orange) explains approximately 89% of the interannual variance of the ECCO estimate (blue). This indicates that the assumptions involved in the adjoint-based reconstruction (e.g., stationary linear response) are reasonable. Accounting for the dependence of adjoint sensitivities on seasonally varying ocean state

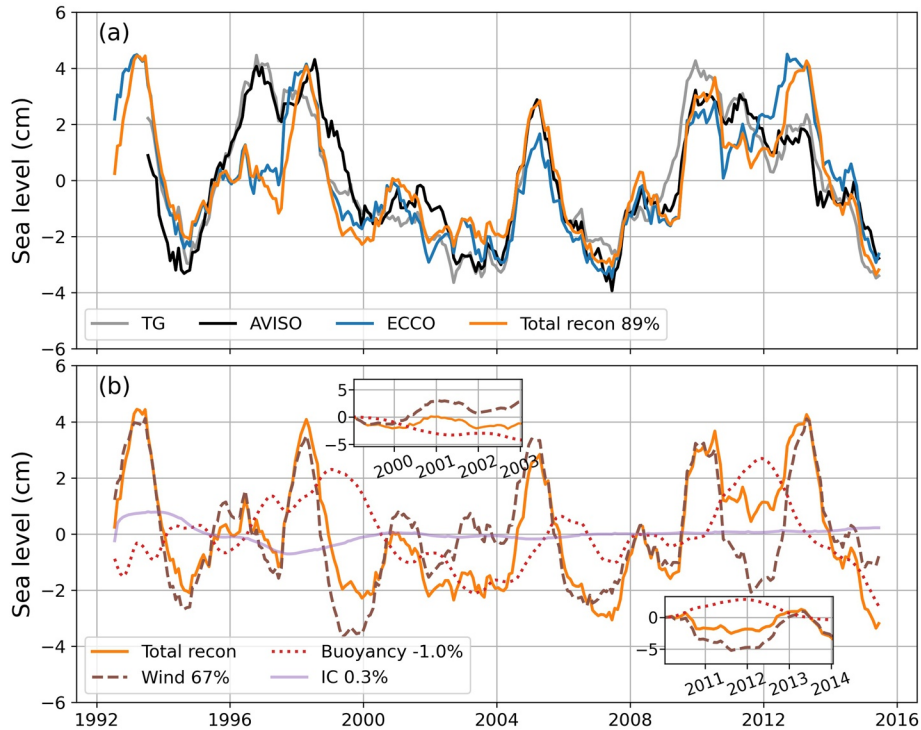

Figure 2. (a) Nantucket SLA from tide gauge (gray), AVISO (black), ECCO (blue), and adjoint-based sea-level reconstruction (orange) using both wind stress and buoyancy forcings plus the contribution of adjustment to initial state. The number (89%) in the legend is the percentage variance of ECCO SLA (blue) explained by the total reconstructed SLA (orange). (b) The total reconstructed SLA (orange; same as in panel (a)) and individual reconstruction using wind stress (dashed), buoyancy forcing (dotted), and the contribution of adjustment to initial state (purple). The numbers are the percentage variance of the total reconstructed SLA (orange) explained by each of these three factors. The two insets show reconstructed SLA for 1999–2002 and 2010–2013. All time series are 13-month low-pass-filtered with the respective mean seasonal cycle and linear trend removed. The curves are referenced to their corresponding time mean, except that those in the insets are relative to January 1999 and January 2010, respectively. Units are in cm.

(e.g., Verdy et al., 2014) may increase the variance explained beyond 89%, but at much higher computational cost because it requires 11 more multi-decadal adjoint sensitivity runs.

Having established that Equation 1 can reconstruct most of the interannual variability of Nantucket sea level represented in ECCO, we next quantify the contributions by wind stress and buoyancy forcings (Figure 2b). Wind stress (dashed) is the largest contributor, explaining 67% of the interannual variance of the reconstructed Nantucket sea level. This confirms previous studies suggesting that wind forcing is the dominant contributor to sea-level variations along the US northeast coast (Andres et al., 2013; Piecuch et al., 2016, 2019; Piecuch & Ponte, 2015; Woodworth et al., 2014). A prominent example is during 2009–2010 when the 5-cm increase of sea level is almost completely due to wind forcing. Goddard et al. (2015) found that the increase of sea level along the US northeast coast during 2009–2010 is consistent with the northeasterly wind stress anomaly during the same period that causes anomalous onshore Ekman transport.

Although sizable, buoyancy forcing contribution (dotted) does not formally explain much variance of the overall interannual variation of Nantucket sea level during the 1992–2015 period (−1%). However, the difference in variance explained by the total reconstruction (89%) and wind stress contribution (67%) is largely due to buoyancy forcing which can be as important as wind stress during certain years. For example, during 2010–2013 wind stress causes a 5-cm decrease of sea level, but it is offset by a 3-cm increase of sea level due to buoyancy forcing (inset on the right of Figure 2b). During 1999–2002, the 3-cm increase of sea level due to wind stress is offset by a 4-cm decrease due to buoyancy forcing (inset on the left of Figure 2b). Buoyancy forcing also appears to be more important at lower frequencies than wind forcing. The reconstructions by wind and buoyancy forcings have partial compensation with weak but significant anticorrelation ($r = -0.26$). Note that the explained variances by individual forcing contributions are not additive because forcings may covary. Such covariation makes it difficult

Table 1
Standard Deviation (σ; in cm) of Reconstructed Nantucket Sea Level and Correlation Coefficient (r) Between Total Reconstruction and the Reconstruction Using an Individual Forcing

Reconstruction	σ	r
Total	1.94	1
Wind	1.88	0.83
Buoyancy	1.19	0.30

to separate the forcing contributions using traditional covariance-based analyses (e.g., regression). A negative explained variance of one variable by another occurs when they are anticorrelated or the ratio of the latter's standard deviation (σ) to the former's is twice larger than r (see Fukumori et al., 2015). Table 1 lists σ of reconstructed sea-level and r between total reconstruction and the reconstructions by individual forcings. The fact that wind stress and buoyancy forcing together explain 97% of the variance of Nantucket sea level even though buoyancy forcing alone does not explain any interannual variance suggests the importance of buoyancy forcing.

The contribution of the anomalies in the initial condition (purple in Figure 2b) quantifies the effect of sea-level adjustment to the initial state of the ECCO model that is independent from the effects of subsequent forcings. The initial condition's contribution is obtained by taking the difference between the ECCO solution and the same simulation in which the model's initial conditions are replaced by its 1992–2015 time-mean ocean state. The variance explained by the initial state is close to zero and mostly affects sea level before 2000.

4. Local and Remote Forcing Contributions

We further investigate the local and remote contributions of wind and buoyancy forcings. By excluding the spatial summation in Equation 1, we obtain the contribution of a forcing at each location to Nantucket sea level. We then compute the fraction of Nantucket interannual sea-level variance explained by reconstructed SLA using wind stress or buoyancy forcing at each location. The resultant maps, referred to as the forcing influence maps, are shown in Figure 3. Similar to adjoint sensitivities of wind stress (Figure 1), wind stress contribution (Figure 3a) is seen to be mainly local, with the largest contribution from the GoM and Scotian Shelf northeast of Nantucket. Moreover, wind stress contribution is largely confined to the shelf and almost entirely northeast of Nantucket. Outside the large and positive local influence region, there is little contribution by wind stress.

Buoyancy forcing, on the other hand, has contributions covering a much broader region northeast of Nantucket, including remote areas in the subpolar North Atlantic (Figure 3b). There is a local positive contribution from the GoM and Scotian Shelf. In the subpolar region, there are positive remote contributions by buoyancy forcing over the Labrador Sea, the western subpolar gyre, and the southeastern Greenland Shelf. There are also weak positive contributions farther upstream along the eastern coasts of the Atlantic Ocean and Nordic Seas. Values of negative variance explained are found for buoyancy forcing from the eastern subpolar gyre, the continental slopes of Grand Banks and Flemish Cap, and the Gulf of St. Lawrence. There are also noticeable negative values of explained

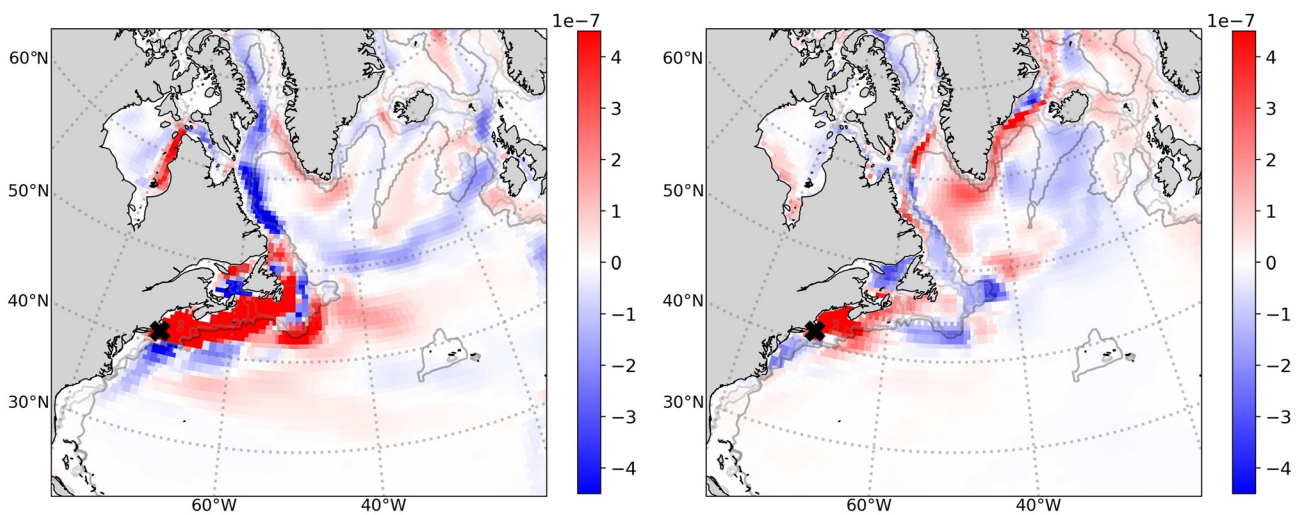

Figure 3. Fractions of variance of the total reconstructed Nantucket interannual SLA explained by reconstructed SLA using (a) wind stress and (b) buoyancy forcing per unit area (km^{-2}) at each location. Contours are isobaths of 200, 700, and 2,000 m (dark gray).

Table 2
Percentage Variance of Total Reconstructed SLA Explained by the Reconstructed SLA Using Wind Stress and Buoyancy Forcing From Various Forcing Regions

Forcing	Region name	Description	Explained variance (σ; r)
Wind	Local (Gulf of Maine)	71°–66°W, 40°–45°N, 0–2,000 m	48% (0.84; 0.77)
	Regional	80°–60°W, 35°–45°N, 0–2,000 m	66% (1.3; 0.83)
	Remote	All areas outside the regional forcing box	27% (0.87; 0.53)
	Labrador Sea	65°–45°W, 50°–70°N	−15% (0.46; −0.19)
Buoyancy	Local (Gulf of Maine)	71°–66°W, 40°–45°N, 0–2,000 m	2.6% (0.54; 0.19)
	Regional	80°–60°W, 35°–45°N, 0–2,000 m	2.7% (0.58; 0.20)
	Remote	All areas outside the regional forcing box	8.5% (0.79; 0.31)
	Labrador Sea	65°–45°W, 50°–70°N	0.0% (0.48; 0.12)

Note. The standard deviation (σ) of total reconstructed SLA is 1.9 cm. The numbers in parenthesis are the standard deviation (cm) of the reconstruction by a particular forcing from a specified region and the correlation coefficient (r) between the total and specific reconstructed SLAs.

variance from the Labrador and Newfoundland shelves that are sandwiched between positive values from the Labrador Sea and coastal regions.

Frederikse et al. (2017) identified a strong correlation between decadal changes of steric height in the subpolar North Atlantic and the sea level along the US northeast coast. The region with large contribution of remote buoyancy forcing identified in our study is roughly over the same region where they found good correlation between subpolar steric height and sea level along the US northeast coast. Our results corroborate their hypothesis that sea-level variations in the subpolar gyre and the US northeast coast can both be influenced by subpolar buoyancy forcing, with our results demonstrating this causality. Our results also suggest that subpolar buoyancy forcing explains only 10% of the interannual variance of Nantucket sea level.

The contributions from local and remote forcings can be quantified by the variance of the total reconstructed SLA explained by each forcing from various forcing regions (defined in Table 2 and Figure 4; Table 2 also has other statistics, σ and r). Here the local forcing region is defined as the GoM with depths shallower than 2,000 m. We also consider a larger regional forcing box, encompassing the smaller local forcing box as well as the Mid-Atlantic Bight to the south and the Scotian Shelf to the north. Any contributions outside the regional forcing box are considered as remote forcing contributions.

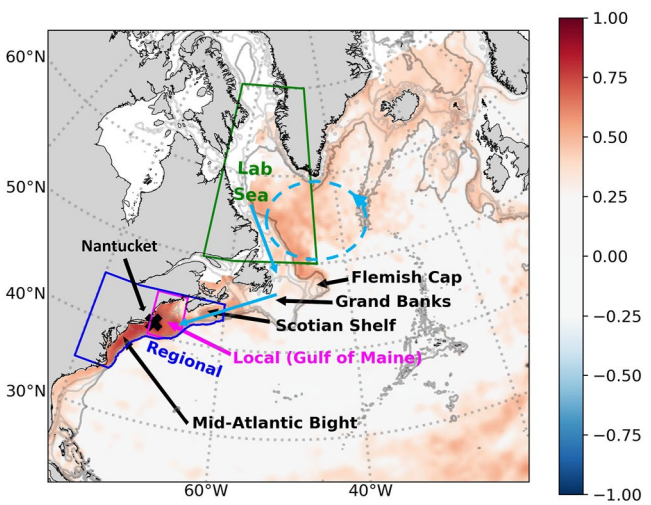

Figure 4. Forcing regions shown in a map of the correlation coefficient between the monthly-mean AVISO SLA near Nantucket Island (denoted as X) and that at each grid point. See Table 2 for definitions of the forcing regions. The remote forcing region is defined as all areas outside the regional forcing box (in blue). The dashed oval is a schematic illustration of the subpolar gyre and its counterclockwise circulation (as designated by the arrow on its perimeter). The two straight arrows are schematic illustrations of the Labrador Current and shelf break currents. Contours are isobaths of 200, 700, and 2,000 m (dark gray). The sea level is the same as used in Figure S1.

Table 2 summarizes the variance of the total reconstructed SLA explained by wind and buoyancy forcings from the various regions defined above. For winds, the GoM (local forcing region) is the main contributor, explaining about 48% of the variance of the total reconstructed Nantucket sea level. The regional wind contributions from the GoM, Mid-Atlantic Bight, and Scotian Shelf account for 66% of the variance. Remote winds explain about 27% of the variance, smaller than the local and regional wind contributions. In contrast, remote buoyancy forcing contribution is larger than local buoyancy forcing contribution, explaining 8.5% and 2.6% of the variance of the total reconstructed SLA respectively. Our causal analysis indicates that local wind stress is the main contributor to sea level change along the US northeast coast.

Figure 5 shows the reconstructed sea-level time series using wind stress (Figure 5a) and buoyancy forcing (Figure 5b) from various forcing regions (Table 2). The numbers in the figure legend are the variance of the reconstructed SLA using wind stress (Figure 5a) and buoyancy forcing (Figure 5b) explained by the reconstruction from each forcing region. For wind stress, the local forcing box explains 58% of the variance of the wind reconstruction, more than that of the remote forcing region (49%). That the local wind contribution is larger than the remote wind contribution is consistent with what is shown in Table 2. The wind stress contribution from the Labrador Sea is

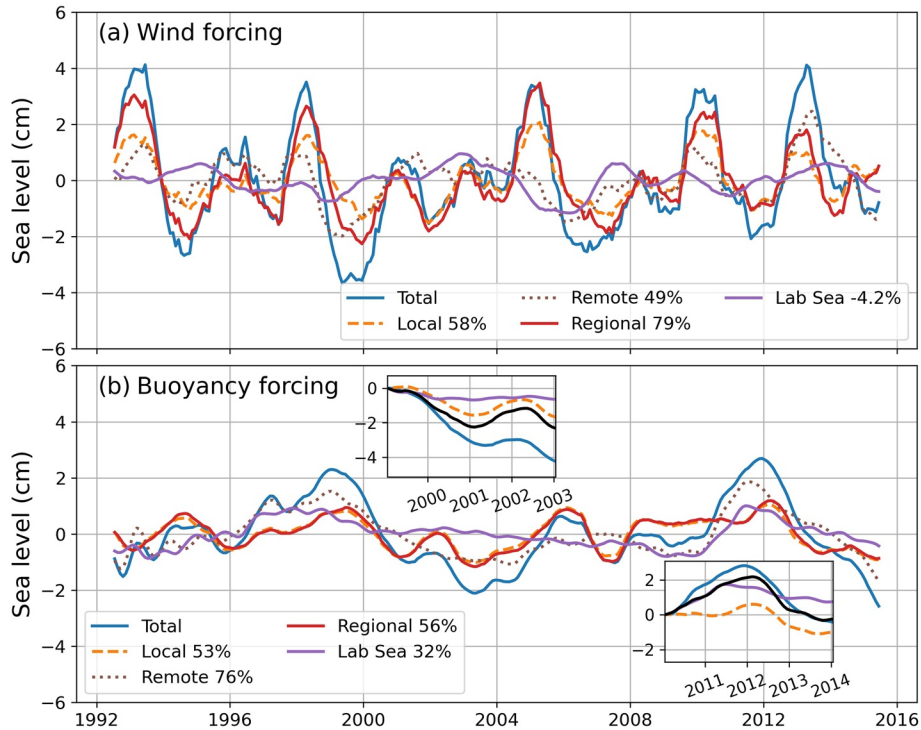

Figure 5. Reconstructed SLAs (cm) using a particular forcing in a specific forcing region for (a) wind stress and (b) buoyancy forcing. The individual curves are reconstructed SLAs from the globe (blue), local (dashed), remote (dotted), regional (red), and Labrador Sea (purple) forcing regions. See text and Table 2 for definitions of the forcing regions. The numbers are percentage explained variance of reconstructed SLA using a particular forcing over a specific region. The insets show reconstructed SLAs for 1999–2002 and 2010–2013. Also shown in the inset is the sum (black) of reconstructed SLAs from the local forcing box (dashed) and Labrador Sea (purple). All curves are relative to the corresponding time mean, except that those in the insets are relative to January 1999 and January 2010.

negative (−4.2%). Also, the magnitude of reconstructed SLA from wind stress over the Labrador Sea is small (the largest being about 1 cm) compared with the 4-cm magnitude of that using wind stress from all regions. Reconstructed SLA using wind stress from the Labrador Sea is uncorrelated to that from all forcing regions (r being close to zero). The lack of wind stress contribution from the Labrador Sea found in this study differs from what was hypothesized by Andres et al. (2013) based on the anticorrelation of wind stress curl in the Labrador Sea with North-America coastal sea level. The ECCO wind stress curl is indeed significantly anticorrelated with Nantucket sea level ($r = -0.46$), similar to Andres et al. (2013). However, our causal analysis presented above shows that Labrador Sea wind stress curl is not an important driver of sea-level variation along the US northeast coast.

For reconstructed SLA using buoyancy forcing, local and remote forcings explain 53% and 76% of the variance, respectively. That the remote buoyancy forcing is larger than the local buoyancy forcing is also consistent with what the explained variance of the total reconstructed SLA indicates (Table 2).

5. Enhanced Buoyancy Contribution During 2010–2013 and 1999–2002

While wind contribution is generally larger than the buoyancy forcing contribution, the latter can be as important as the former in some years (Figure 2b), most notably during 2010–2013 and 1999–2002. Here, we further investigate where the buoyancy contribution came from during the two time periods. The contributions of local and remote buoyancy forcing for 2010–2013 and 1999–2002 are illustrated in the insets of Figure 5b, where the time series are the same as the curves in Figure 5b but with the anomalies computed relative to January 2010 and January 1999, respectively.

For 2010–2013, there was about 3-cm of SLR from 2010 to early 2012. The main contributor is from the Labrador Sea and starts in 2010. There was a record low of ocean heat loss in the Labrador Sea during 2008–2010,

which would create a positive sea-level change along the US northeast coast (Goddard et al., 2015). Adjoint sensitivities (Figures 1a–1h) and a forward perturbation experiment later in the study (Section 6.1.1) indicate that a perturbation of buoyancy forcing in the Labrador Sea takes 2–3 years to affect Nantucket sea level. Therefore, the record low of ocean heat loss in the Labrador Sea during 2008–2010 is expected to cause a sea-level rise near Nantucket during 2010–2012.

The buoyancy forcing contribution from the Labrador Sea peaks in mid-2011. However, the local buoyancy forcing contribution starts to increase around the same time and extends through the first half of 2012. The local contribution seems to be caused by the marine heat wave event during 2011–2012 that generated a record warm sea surface temperature (SST) not seen in past 150 years (Chen et al., 2014, 2015). Local buoyancy forcing causes about 1-cm increase in Nantucket sea level and is almost completely due to heat flux forcing (not shown), consistent with the impact of the marine heat wave event.

There is also another event during 1999–2002 when reconstructed SLA due to buoyancy decreases by more than 4 cm. The buoyancy forcing from the GoM and Scotian Shelf causes about 1.9 cm decrease, while the remote buoyancy forcing from the Grand Banks, Labrador Sea and the subpolar gyre caused about 1.3-cm decrease.

The results in this section suggest that Nantucket sea level may be partly predictable a couple years into the future in some years. The forcing influence map (Figure 3b) and the sensitivity maps due to heat and freshwater fluxes (Figures 1a–1h) illustrate where and when buoyancy forcing affects the interannual variations of Nantucket sea level. In particular, the remote buoyancy forcing from the subpolar North Atlantic, especially the large positive influence region (red color in Figure 3b), can have a significant effect on Nantucket sea level a few years later.

6. Perturbation Experiments

To investigate how forcing affects Nantucket sea level, we further conduct forward forcing perturbation experiments similar to Fukumori et al. (2015). Analysis of the forward model evolutions in response to the selected forcing perturbations sheds light on the associated oceanic processes and time scales. We present results related to remote buoyancy forcing in Section 6.1 and wind stress in Section 6.2. Note that the forcing perturbation experiments described in this section do not use the bulk-formula forcing formulation. The bulk formulae act to "restore" the surface ocean to a certain value based on atmospheric states, which presumably would make the buoyancy anomalies dampen away more quickly. Future efforts investigating potential impact of using the bulk-formula methodology on evolution of the perturbed ocean state would be of interest.

6.1. Remote Buoyancy Forcing

The buoyancy forcing influence map (Figure 3b) provides a guidance for the forcing perturbations. Here we conducted three forward model sensitivity experiments by perturbing the remote buoyancy forcing in the subpolar gyre south of Greenland (Section 6.1.1), along the continental shelf in the Labrador Sea (Section 6.1.2), and near the Flemish Cap (Section 6.1.3). The buoyancy forcing in the first two regions is associated with relatively large positive variance explained for Nantucket sea level, while that in the third region is associated with negative variance explained.

6.1.1. Subpolar North Atlantic

We perturb the heat flux in the subpolar North Atlantic (Figure 6a) where there are large positive contributions by remote buoyancy forcing, specifically, the deep ocean (>2,000 m) between 65°–45°W and 50°–60°N that has explained variance of Nantucket sea level larger than 2.5×10^{-7} km^{-2} (see Figure 3b). The prescribed heat flux perturbation increases linearly over the course of one week reaching a maximum magnitude of 5 W m^{-2} at 12 Z of 9 December 1992, and then decreases linearly to zero over the course of one week.

The monthly-mean perturbed SLA, computed as the sea level difference between the perturbed run and the reference run (i.e., ECCO V4r3), indicates that the positive heat flux perturbation creates an initial SLA that is predominantly positive due to local thermosteric effect. The positive anomaly first rotates counterclockwise while spreading to a larger region of the subpolar gyre due to the effect of the circulation. Figure 6b shows SLA about 1 month after the initial heat flux perturbation is applied. The dominant feature is a region of large positive anomaly (red color) not very far away from the region with initial heat flux perturbation. There are small

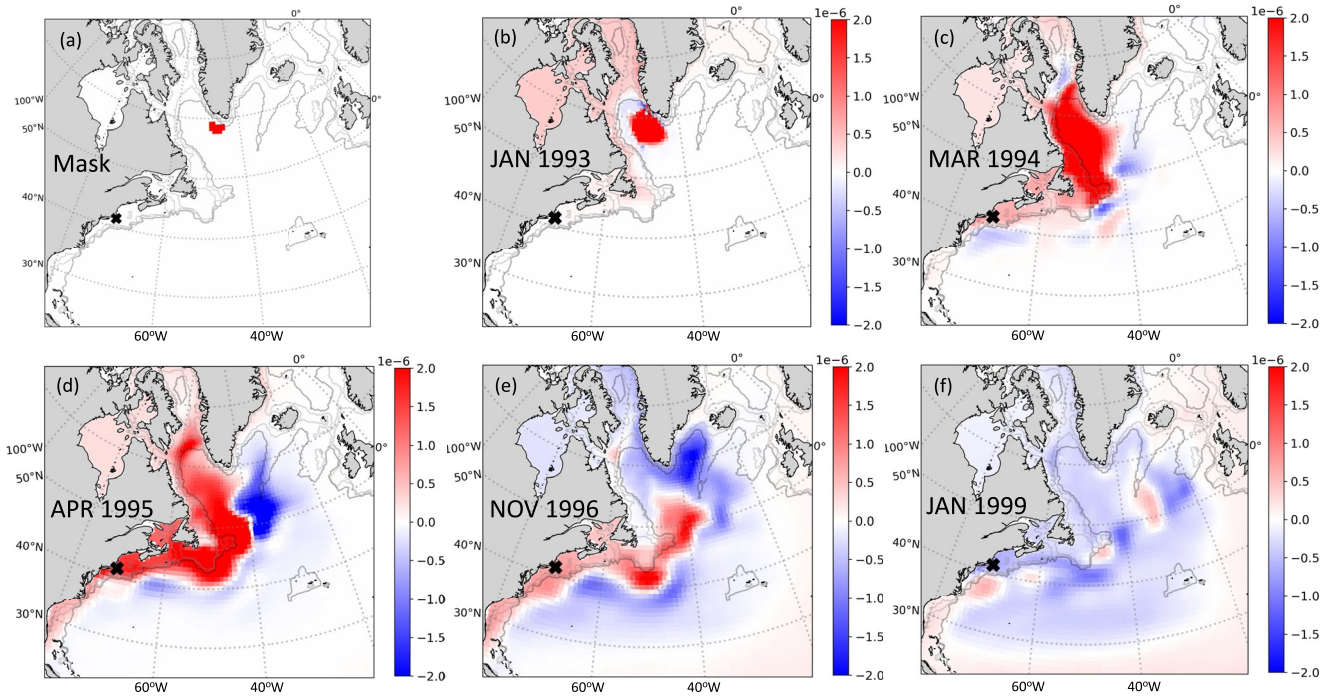

Figure 6. (a) Mask (in red) for a 2-week heat flux perturbation centered at 12Z, 9 December 1992 that is applied in the subpolar North Atlantic (see text). (b)–(f) The resultant monthly-average SLA (m) in January 1993 (b), March 1994 (c), April 1995 (d), November 1996 (e), and January 1999 (f). Nantucket is denoted by X.

positive SLAs in distant regions such as Hudson Bay and a large swath of continental shelves along the east coast of North America. Although not visibly noticeable from the map, the time series of perturbed Nantucket SLA suggests that very weak signals can actually reach Nantucket within 1 month (cyan curve in Figure 7). This quick Nantucket sea-level response to the heat flux perturbation in the subpolar North Atlantic is likely due to coastally trapped waves with typical speeds around 2–3 m s^{-1} at high latitudes that would take a few weeks to propagate from the perturbed subpolar North Atlantic to reach Nantucket (Meyers et al., 1998; also see Figure 1 of Hughes et al., 2019).

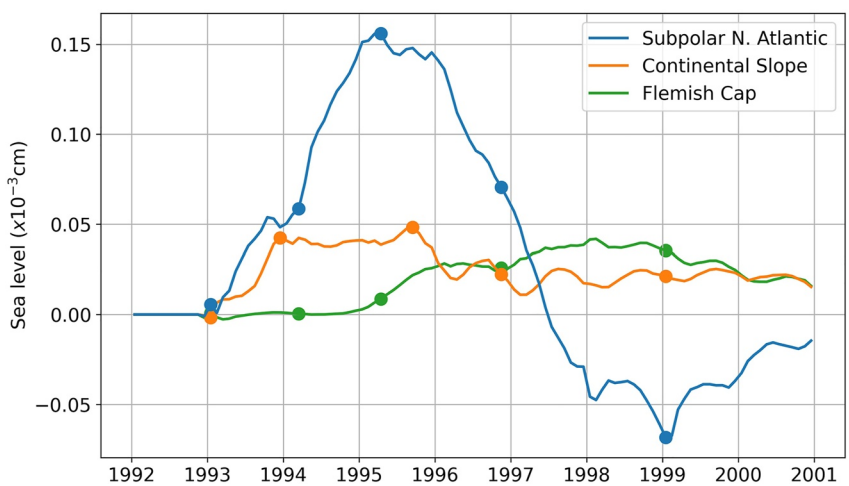

Figure 7. Time series of monthly-mean perturbed SLA ($\times 10^{-3}$ cm) at Nantucket for heat flux perturbation applied to the subpolar North Atlantic Ocean (cyan), over the continental slope of the Labrador Sea (orange), and over Flemish Cap (green). Dots correspond to the time instances for panels (b)–(f) of Figures 6, 8 and 9.

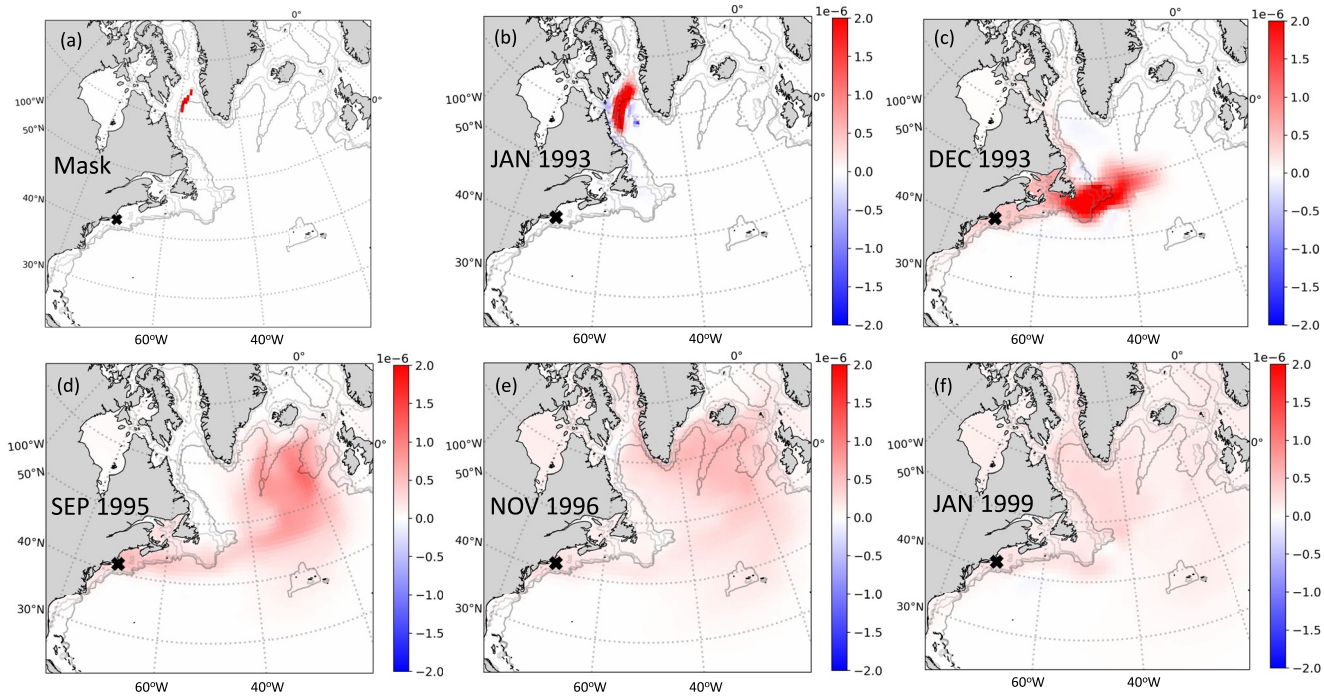

Figure 8. Same as Figure 6, but for the continental shelf of the Labrador Sea. (a) Mask (in red). (b)–(f) The resultant monthly-average SLA (m) in January 1993 (b), December 1993 (c), September 1995 (d), November 1996 (e), and January 1999 (f).

While coastally trapped waves can cause rapid sea level variations thousands of kilometers away (e.g., Johnson & Marshall, 2002; Roussenov et al., 2008), the majority of the positive SLA due to positive heat flux perturbation in the subpolar North Atlantic reaches Nantucket via what appears to be slow advective processes during 1994–1996. After moving westward reaching the continental slope in a month (Figure 6b), the SLA further spreads southward, likely via the Labrador Current. In about 15 months, the anomaly reaches the Grand Banks (Figure 6c). The SLA further spreads southwestward along the shelf. The perturbed SLA at Nantucket reaches the maximum response in about 2 years (Figure 6d), remaining around the same magnitude for about 1 year (Figure 7) and then gradually decaying thereafter (Figures 6e and 6f). The adjustment of SLA by the slow advective process is similar to what was found by Hsieh and Bryan (1996) using a simple shallow-water model.

6.1.2. Continental Slope

We conduct a second experiment over the continental shelf in the Labrador Sea where explained variance is also large (Figure 3b). The same perturbation as in the first experiment is applied to the region between 65°–55°W and 60°–70°N where the values of explained variance in Figure 3b are larger than 2.5×10^{-7} km^{-2} (Figure 8a).

The positive heat flux perturbation creates positive SLA that quickly spreads to the shelf (Figure 8b), moves southward (Figure 8c), and further expands to the shelf and the subpolar North Atlantic (Figures 8d–8f). SLA at Nantucket (orange curve in Figure 7) reaches a plateau in about 1 year (December 1993) and stays on approximately the same magnitude for about 18 months (through June 1995). The anomaly further increases to the peak in September 1995 and then reduces over time. The perturbed SLA at Nantucket reaches a plateau in 1 year in this experiment as opposed to be 2 years in the first experiment because the perturbed heat flux in this experiment, being over the continental slope, is closer to the Labrador Current that carries the perturbed sea level signal.

6.1.3. Flemish Cap

We also conduct a third experiment on Flemish Cap where explained variance is negative. The same perturbation to heat flux is applied over Flemish Cap where the explained variance in Figure 3b is smaller than -2×10^{-7} km^{-2} (Figure 9a).

As in the other two experiments, the positive heat flux perturbation first generates positive SLA. In 1 month, the positive SLA propagates northeastward (away from Nantucket) and barely has any effect on Nantucket sea level

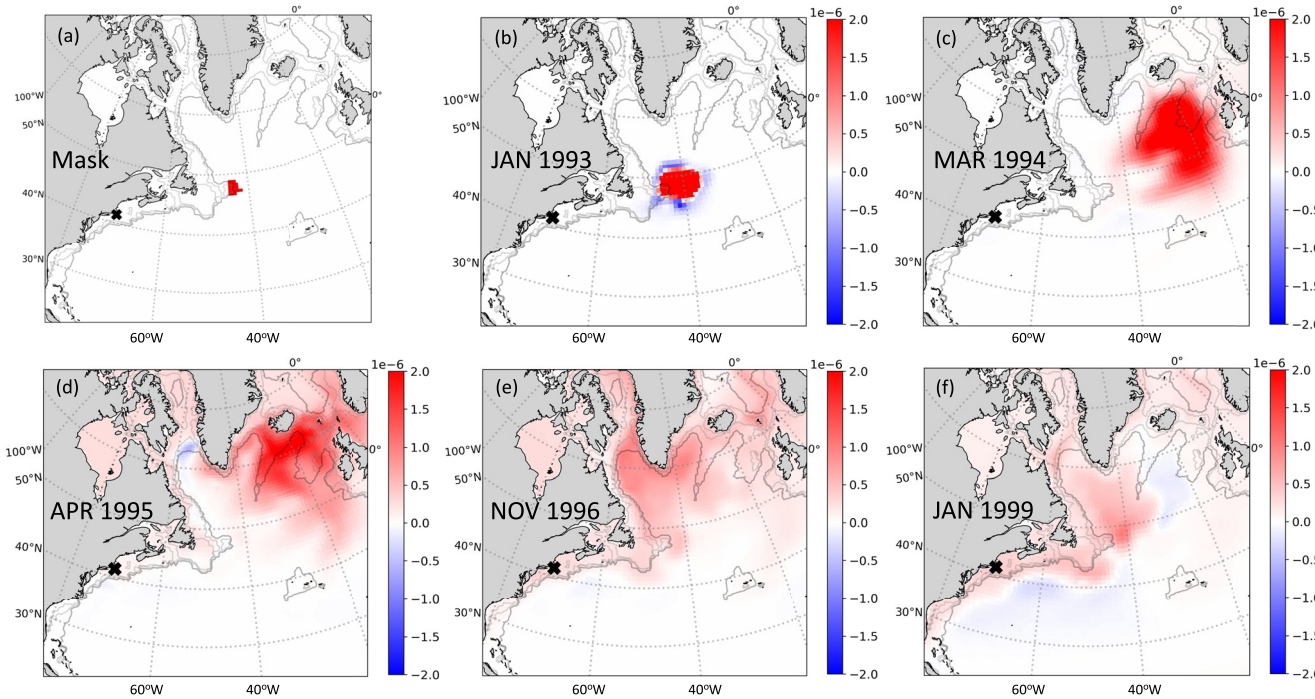

Figure 9. Same as Figure 6, but for Flemish Cap (see text). (a) Mask (in red). (b)–(f) The resultant monthly-average SLA (m) in January 1993 (b), March 1994 (c), April 1995 (d), November 1996 (e), and January 1999 (f).

(Figure 9b). It subsequently spreads to a larger area to the northeast while rotating counterclockwise (Figure 9c) and gradually occupies the whole subpolar North Atlantic and Nordic Seas (Figures 9d and 9e). After 2 years, the positive sea level signal starts affecting Nantucket sea level (Figures 9e and 9f). Time series of the perturbed SLA at Nantucket shows very small values for over 2 years after the heat flux perturbation was applied (green curve in Figure 7). Nantucket SLA eventually increases and reaches its maximum after 5 years, much longer than the other two experiments. The negative explained variance near Flemish Cap (Figure 3b) thus can be attributed to the much longer time scales of the anomaly as it travels and dissipates around the subpolar gyre, thereby causing a response of Nantucket sea level that is not coherent with the dominant interannual signal at Nantucket.

6.2. Wind Stress

Sensitivities to wind stress also show some interesting patterns. For instance, there is a dipole pattern for meridional wind stress over George Banks (Figure 1p). We explore it by conducting similar perturbation experiments to meridional wind stress over the western (Figure 10a) and eastern (Figure 10d) Grand Banks, respectively. The perturbated regions were chosen where the normalized sensitivities over the Grand Banks (Figure 1p) are larger than 0.27 and less than −0.34 for the two experiments. Same as in the previous three experiments, a positive perturbation with a maximum magnitude of 0.05 N m^{-2} is applied over a 2-week period in December 1992.

The two perturbations initially generate SLAs with opposite signs, likely because Ekman transport due to perturbation in meridional wind stress moves water toward and away from the shallow region of Grand Banks, respectively (Figures 10b and 10e). The anomaly quickly propagates counterclockwise along the shelf as coastally trapped waves, with SLA at Nantucket reaching its maximum within 1–2 months (Figure 10g). The anomaly dissipates more rapidly than in the three heat flux perturbation experiments (compare Figure 10g vs. Figure 7). Although the majority of SLA dissipates quickly, some small SLA persists for a long time, probably propagating via higher-mode coastally trapped waves and through advective-diffusive processes. Figures 10c and 10f show SLA 3 years after the initial perturbation. SLA now occupies the whole North Atlantic with a maximum magnitude three orders smaller than that of the initial SLA. SLAs at Nantucket are positive and negative for the two experiments, consistent with the dipole pattern in the sensitivity map (Figure 1p).

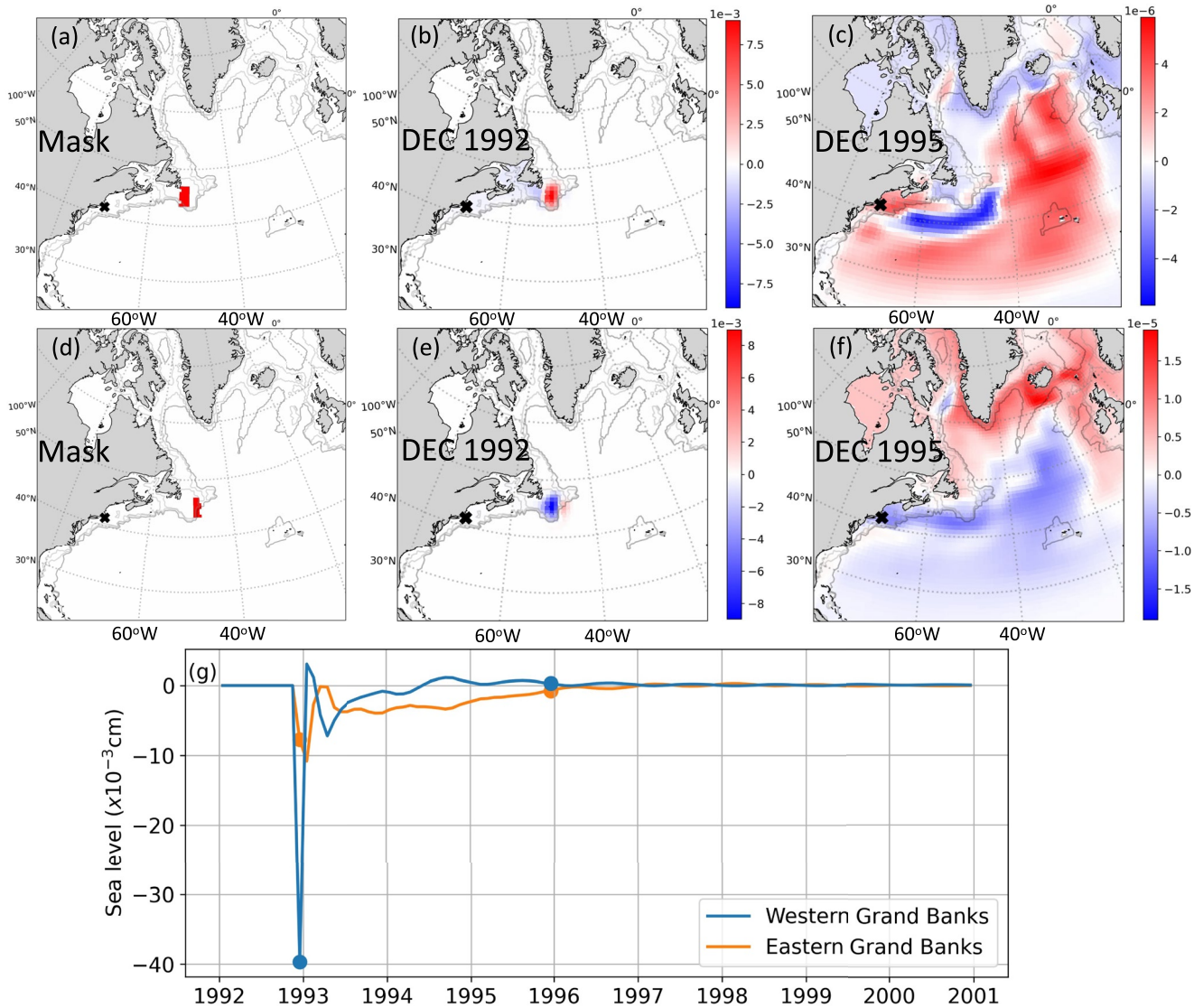

Figure 10. Same as Figure 6, but for perturbations applied to meridional wind stress over (a)–(c) western and (d)–(f) eastern Grand Banks, respectively. Panels (a) and (d) are the mask, while the other maps are SLAs (m). (g) Respective time series of SLA at Nantucket, same as in Figure 7.

7. Concluding Remarks

We conducted a causal analysis to quantify the impacts of local and remote atmospheric forcings on interannual variations of Nantucket sea level. We first reconstructed Nantucket sea-level variations through the convolution of forcing anomalies with sea-level sensitivities to forcings computed using the adjoint of the ECCO model. We then decomposed the convolution into contributions by local and remote wind and buoyancy forcings. Wind forcing explains 67% of the Nantucket interannual sea-level variance, while wind and buoyancy forcing together explain 97% of the variance.

Wind stress contribution is mainly local, from the GoM and Scotian Shelf northeast of Nantucket. Wind stress from the GoM alone explains 48% of the Nantucket sea-level variance. If regional wind stress from the Mid-Atlantic Bight to the south and the Scotian Shelf to the north are included, the explained variance increases to 66%. Remote wind stress from outside the three aforementioned regions explains only 27% of the interannual variance of Nantucket sea level.

Remote buoyancy forcing explains 8.5% of Nantucket interannual sea-level variance, larger than the 2.6% variance explained by local buoyancy forcing. Although buoyancy forcing contribution is overall smaller than wind

contribution, it can be comparable to wind contribution in some years (e.g., 1999–2002 and 2010–2013). Remote buoyancy forcing from the subpolar North Atlantic can significantly influence Nantucket sea level a few years later, providing a source of predictability for Nantucket sea-level variations. Forward perturbation experiments indicate that the remote buoyancy forcing affects the Nantucket sea level mainly via slow advective ocean processes, although coastally trapped waves can cause rapid Nantucket sea level response in a few weeks.

The results of our causality analysis (a) confirm the dominant contribution of local winds suggested by most previous studies that were based on correlation analysis or simplified models, (b) validate a hypothesis that subpolar-gyre buoyancy forcing plays a role in sea-level variations along the US northeast coast, and (c) nullify a correlation-based hypothesis that winds over the Labrador Sea are an important driver of sea-level variation along the US northeast coast. Our results about the relative contributions of different forcings and regions also provide useful information to evaluate climate models and to improve statistical or machine-learning methods for sea-level prediction for the US northeast coast.

Future investigations beyond this study include forcing contributions to Nantucket sea-level variations on decadal-and-longer time scales, the effect of adjoint-sensitivity dependence on the seasonally varying ocean state, and similarity and difference in forcing mechanisms for sea-level variations in the US southeast coast (e.g., Volkov et al., 2019) and those in the US northeast coast. Future effort using ECCO Version 4 Release 4, which has air-pressure loading forcing, and its adjoint would allow the inclusion of surface pressure effect in the attribution analysis.

Data Availability Statement

This study uses the following data: ECCO V4r3 (https://ecco.jpl.nasa.gov/drive/files/Version4/Release3), tide gauge (https://www.psmsl.org/data/obtaining/rlr.monthly.data/1111.rlrdata), and AVISO (https://resources.marine.copernicus.eu/product-detail/SEALEVEL_GLO_PHY_L4_MY_008_047/INFORMATION). The adjoint sensitivity, forcing, and reconstruction script can be found at https://ecco.jpl.nasa.gov/drive/files/Version4/Release3/other/research/Nantucket_sea_level.

Acknowledgments
This research was carried out in part at the Jet Propulsion Laboratory, California Institute of Technology, under a contract with the National Aeronautics and Space Administration (80NM0018D0004). CGP was supported by NASA Sea Level Change Team awards 80NSSC20K1241 and 80NM0018D0004.

References

Andres, M., Gawarkiewicz, G. G., & Toole, J. M. (2013). Interannual sea level variability in the western North Atlantic: Regional forcing and remote response. *Geophysical Research Letters*, *40*, 5915–5919. https://doi.org/10.1002/2013GL058013

Campin, J. M., Marshall, J., & Ferreira, D. (2008). Sea ice-ocean coupling using a rescaled vertical coordinate z. *Ocean Model*, *24*, 1–14. https://doi.org/10.1016/j.ocemod.2008.05.005

Chen, K., Gawarkiewicz, G. G., Kwon, Y.-O., & Zhang, W. G. (2015). The role of atmospheric forcing versus ocean advection during the extreme warming of the Northeast U.S. continental shelf in 2012. *Journal of Geophysical Research: Oceans*, *120*, 4324–4339. https://doi.org/10.1002/2014JC010547

Chen, K., Gawarkiewicz, G. G., Lentz, S. J., & Bane, J. M. (2014). Diagnosing the warming of the northeastern U.S. Coastal Ocean in 2012: A linkage between the atmospheric jet stream variability and ocean response. *Journal of Geophysical Research: Oceans*, *119*, 218–227. https://doi.org/10.1002/2013JC009393

Chen, N., Han, G., & Yan, X.-H. (2020). Similarity and difference in interannual sea level variations between the Mid-Atlantic Bight and the Nova Scotia coast. *Journal of Geophysical Research: Oceans*, *125*, e2019JC015919. https://doi.org/10.1029/2019JC015919

Forget, G., Campin, J.-M., Heimbach, P., Hill, C. N., Ponte, R. M., & Wunsch, C. (2015). ECCO version 4: An integrated framework for non-linear inverse modeling and global ocean state estimation. *Geosci. Model Dev*., 8, 3071–3104. https://doi.org/10.5194/gmd-8-3071-2015

Forget, G., & Ponte, R. M. (2015). The partition of regional sea level variability. *Progress in Oceanography*, *137*, 173–195. https://doi.org/10.1016/j.pocean.2015.06.002

Frederikse, T., Simon, K., Katsman, C. A., & Riva, R. (2017). The sea-level budget along the northwest Atlantic coast: GIA, mass changes, and large-scale ocean dynamics. *Journal of Geophysical Research: Oceans*, *122*, 5486–5501. https://doi.org/10.1002/2017JC012699

Fukumori, I., Menemenlis, D., & Lee, T. (2007). A near-uniform basin-wide sea level fluctuation of the Mediterranean Sea. *Journal of Physical Oceanography*, *37*(2), 338–358. https://doi.org/10.1175/JPO3016.1

Fukumori, I., Wang, O., & Fenty, I. (2021). Causal mechanisms of sea-level and freshwater content change in the Beaufort Sea. *Journal of Physical Oceanography*, *41*(10), 3217–3234. https://doi.org/10.1175/JPO-D-21-0069.1

Fukumori, I., Wang, O., Fenty, I., Forget, G., Heimbach, P., & Ponte, R. M. (2017). *ECCO Version 4 Release 3*. Retrieved from http://hdl.handle.net/1721.1/110380

Fukumori, I., Wang, O., Llovel, W., Fenty, I., & Forget, G. (2015). A near-uniform fluctuation of ocean bottom pressure and sea level across the deep ocean basins of the Arctic Ocean and the Nordic Seas. *Progress in Oceanography*, *134*, 152–172. https://doi.org/10.1016/j.pocean.2015.01.013

Goddard, P. B., Yin, J., Griffies, S. M., & Zhang, S. (2015). An extreme event of sea-level rise along the Northeast coast of North America in 2009–2010. *Nature Communications*, *6*, 6346. https://doi.org/10.1038/ncomms7346

Heimbach, P., Wunsch, C., Ponte, R. M., Forget, G., Hill, C., & Utke, J. (2011). Timescales and regions of the sensitivity of Atlantic meridional volume and heat transport: Toward observing system design. *Deep Sea Research Part II: Topical Studies in Oceanography*, *58*, 1858–1879. https://doi.org/10.1016/j.dsr2.2010.10.065

Hsieh, W., & Bryan, K. (1996). Redistribution of sea level rise associated with enhanced greenhouse warming: A simple model study. *Climate Dynamics*, *12*, 535–544. https://doi.org/10.1007/BF00207937

Hughes, C. W., Fukumori, I., Griffies, S. M., Huthnance, J. M., Minobe, S., Spence, P., et al. (2019). Sea level and the role of coastal trapped waves in mediating the influence of the open ocean on the coast. *Surveys in Geophysics*, *40*, 1467–1492. https://doi.org/10.1007/s10712-019-09535-x

Johnson, H. L., & Marshall, D. P. (2002). A theory for the surface Atlantic response to thermohaline variability. *Journal of Physical Oceanography*, *32*, 1121–1132. https://doi.org/10.1175/1520-0485(2002)032<1121:atftsa>2.0.co;2

Kostov, Y., Johnson, H. L., Marshall, D. P., Heimbach, P., Forget, G., Holliday, N. P., et al. (2021). Distinct sources of interannual subtropical and subpolar Atlantic overturning variability. *Nature Geoscience*, *14*, 491–495. https://doi.org/10.1038/s41561-021-00759-4

Little, C. M., Hu, A., Hughes, C. W., McCarthy, G. D., Piecuch, C. G., Ponte, R. M., & Thomas, M. D. (2019). The relationship between U.S. East Coast sea level and the Atlantic meridional Overturning Circulation: A review. *Journal of Geophysical Research: Oceans*, *124*, 6435–6458. https://doi.org/10.1029/2019JC015152

Little, C. M., Piecuch, C. G., & Ponte, R. M. (2021). North American East Coast sea level exhibits high power and spatiotemporal complexity on decadal timescales. *Geophysical Research Letters*, *48*, e2021GL093675. https://doi.org/10.1029/2021GL093675

Liu, C., Liang, X., Ponte, R. M., Vinogradova, N., & Wang, O. (2019). Vertical redistribution of salt and layered changes in global ocean salinity. *Nature Communications*, *10*, 3445. https://doi.org/10.1038/s41467-019-11436-x

McCarthy, G. D., Haigh, I. D., Hirschi, J. J.-M., Grist, J. P., & Smeed, D. A. (2015). Ocean impact on decadal Atlantic climate variability revealed by sea-level observations. *Nature*, *521*(7553), 508–510. https://doi.org/10.1038/nature14491

Meyers, S. D., Melsom, A., Mitchum, G. T., & O'Brien, J. J. (1998). Detection of the fast Kelvin wave teleconnection due to El Niño-Southern Oscillation. *Journal of Geophysical Research*, *103*(C12), 27655–27663. https://doi.org/10.1029/98JC02402

Piecuch, C. G., Dangendorf, S., Gawarkiewicz, G. G., Little, C. M., Ponte, R. M., & Yang, J. (2019). How is New England coastal sea level related to the Atlantic meridional overturning circulation at 26°N? *Geophysical Research Letters*, *46*, 5351–5360. https://doi.org/10.1029/2019GL083073

Piecuch, C. G., Dangendorf, S., Ponte, R. M., & Marcos, M. (2016). Annual sea level changes on the North American Northeast Coast: Influence of local winds and barotropic motions. *Journal of Climate*, *29*, 4801–4816. https://doi.org/10.1175/JCLI-D-16-0048.1

Piecuch, C. G., & Ponte, R. M. (2015). Inverted barometer contributions to recent sea level changes along the northeast coast of North America. *Geophysical Research Letters*, *42*, 5918–5925. https://doi.org/10.1002/2015GL064580

Pillar, H. R., Heimbach, P., Johnson, H. L., & Marshall, D. P. (2016). Dynamical attribution of recent variability in Atlantic overturning. *Journal of Climate*, *29*(9), 3339–3352. https://doi.org/10.1175/JCLI-D-15-0727.1

Ponte, R. M., & Piecuch, C. G. (2018). Mechanisms controlling global mean sea surface temperature determined from a state estimate. *Geophysical Research Letters*, *45*, 3221–3227. https://doi.org/10.1002/2017GL076821

Ponte, R. M., Sun, Q., Liu, C., & Liang, X. (2021). How salty is the global ocean: Weighing it all or tasting it a sip at a time? *Geophysical Research Letters*, *48*, e2021GL092935. https://doi.org/10.1029/2021GL092935

Roussenov, V. M., Williams, R. G., Hughes, C. W., & Bingham, R. J. (2008). Boundary wave communication of bottom pressure and overturning changes for the North Atlantic. *Journal of Geophysical Research*, *113*, C08042. https://doi.org/10.1029/2007JC004501

Sallenger, A. H., Doran, K. S., & Howd, P. A. (2012). Hotspot of accelerated sea-level rise on the Atlantic coast of North America. *Nature Climate Change*, *2*, 884–888. https://doi.org/10.1038/nclimate1597

Schloesser, F., Thompson, P. R., & Piecuch, C. G. (2021). Meridional asymmetry in recent decadal sea-level trends in the subtropical Pacific Ocean. *Geophysical Research Letters*, *48*, e2020GL091959. https://doi.org/10.1029/2020GL091959

Smith, T., & Heimbach, P. (2019). Atmospheric origins of variability in the South Atlantic meridional overturning circulation. *Journal of Climate*, *32*, 1483–1500. https://doi.org/10.1175/JCLI-D-18-0311.1

Thompson, K. R. (1986). North Atlantic sea-level and circulation. *Geophysical Journal of the Royal Astronomical Society*, *87*(1), 15–32. https://doi.org/10.1111/j.1365-246X.1986.tb04543.x

Thompson, P. R., & Mitchum, G. T. (2014). Coherent sea level variability on the North Atlantic western boun*dary*. *Journal of Geophysical Research: Oceans*, *119*(9), 5676–5689. https://doi.org/10.1002/2014JC009999

Verdy, A., Mazloff, M. R., Cornuelle, B. D., & Kim, S. Y. (2014). Wind-Driven sea level variability on the California coast: An adjoint sensitivity analysis. *Journal of Physical Oceanography*, *44*(1), 297–318. https://doi.org/10.1175/JPO-D-13-018.1

Volkov, D. L., Lee, S.-K., Domingues, R., Zhang, H., & Goes, M. (2019). Interannual sea level variability along the southeastern seaboard of the United States in relation to the gyre-scale heat divergence in the North Atlantic. *Geophysical Research Letters*, *46*, 7481–7490. https://doi.org/10.1029/2019GL083596

Woodworth, P. L., Maqueda, M. A. M., Gehrels, W. R., Roussenov, V. M., Williams, R. G., & Hughes, C. W. (2017). Variations in the difference between mean sea level measured either side of Cape Hatteras and their relation to the North Atlantic Oscillation. *Climate Dynamics*, *49*, 2451–2469. https://doi.org/10.1007/s00382-016-3464-1

Woodworth, P. L., Maqueda, M. A. M., Roussenov, V. M., Williams, R. G., & Hughes, C. W. (2014). Mean sea-level variability along the northeast American Atlantic coast and the roles of the wind and the overturning circulation. *Journal of Geophysical Research: Oceans*, *119*, 8916–8935. https://doi.org/10.1002/2014JC010520

Woodworth, P. L., Melet, A., Marcos, M., Ray, R. D., Wöppelmann, G., Sasaki, Y. N., et al. (2019). Forcing factors affecting sea level changes at the Coast. *Surveys in Geophysics*, *40*, 1351–1397. https://doi.org/10.1007/s10712-019-09531-1